Eur. Phys. J. D **39**, 227–236 (2006)
DOI: 10.1140/epjd/e2006-00104-5

THE EUROPEAN PHYSICAL JOURNAL D

A density functional theoretic study of novel silicon-carbon fullerene-like nanostructures: $Si_{40}C_{20}$, $Si_{60}C_{20}$, $Si_{36}C_{24}$, and $Si_{60}C_{24}$

A. Srinivasan, M.N. Huda[a], and A.K. Ray[b]

Department of Physics, The University of Texas at Arlington, P.O. Box 19059, Arlington, Texas 76019, USA

Received 6 January 2006 / Received in final form 17 March 2006
Published online 18 May 2006

Abstract. Fullerene-like silicon nanostructures with twenty and twenty-four carbon atoms on the surface of the Si_{60} cage by substitution, as well as inside the cage at various orientations have been studied within the generalized gradient approximation to density functional theory. Full geometry optimizations have been performed without any symmetry constraints using the *Gaussian 03* suite of programs and the LANL2DZ basis set. Thus, for the silicon atom, the Hay-Wadt pseudopotential with the associated basis set is used for the core electrons and the valence electrons, respectively. For the carbon atom, the Dunning/Huzinaga double zeta basis set is employed. Electronic and geometric properties of these nanostructures are presented and discussed in detail. Optimized silicon-carbon fullerene like nanostructures are found to have increased stability compared to the bare Si_{60} cage and the stability depends on the number and the orientation of carbon atoms, as well as on the nature of silicon-carbon and carbon-carbon bonding.

PACS. 73.22.-f Electronic structure of nanoscale materials: clusters, nanoparticles, nanotubes, and nanocrystals

1 Introduction

Experimental and theoretical studies of atomic and molecular clusters continue to be a very active field of research for the last few decades [1–10]. Cage like compact clusters or nanostructures are particularly important as they can be used as building blocks of more stable materials and, in addition to this, the hollow space inside the cage can be doped with different suitable atoms leading to atomically engineered nanostructures with specific scientific and technological applications. For example, well-controlled nanostructures with varying HOMO-LUMO gaps and desired conduction properties can be achieved by controlled doping of atoms in C_{60} [11]. It has also been shown that acceptor $C_{48}B_{12}$ and donor $C_{48}N_{12}$, obtained by doping of C_{60} by substitution, are promising components for molecular rectifiers and nanotube-based transistors among various other applications [12]. The spin property of the doped atom inside the cage can be used as the smallest memory devices for quantum computers. For example a tungsten atom in Si_{12} hexagonal cage is quantum mechanically isolated from outside so that it can preserve its spin state [13].

Silicon is one of the most extensively used semiconductors in the industry and silicon clusters, preferring sp^3 hybridization, have been studied in detail. Ab initio Hartree-Fock (HF) based and density functional theories (DFT) [14–16] have been used to predict the ground state structures of bare silicon clusters. Some of these structures are controversial and there are not enough experimental studies for confirmation of the ground state structures [17]. Discovery of the magically stable C_{60} fullerene cage has prompted scientists to study silicon cage-like fullerene structures, as they can be used as building blocks for fabricating various nanostructures in electronic devices. However, though silicon and carbon belong to same group of periodic table, they exhibit different properties due to differences in their nature of bonding. Carbon clusters (C_n), preferring sp^2 hybridization, have been found to exist in fullerene like structures for n as small as 20 [18,19], whereas for silicon clusters (Si_n) such structures are unstable. Studies on the Si_{60} fullerene cage have yielded a distorted cage structure and Si_{60} fullerene cage is not as stable as C_{60} [20]. Replacing carbon atoms in the C_{60} fullerene cage by silicon atoms has yielded a distorted icosahedral structure [21]. Recently, Matsubara and Massobrio [22] have presented density functional theory based studies of stable highly doped $C_{60-m}Si_m$ hetero-fullerenes. In particular, they have provided clear evidence of stable fullerene-like cage structures for $C_{40}Si_{20}$, $C_{36}Si_{24}$, and $C_{30}Si_{30}$. Core-valence interaction was described by norm-conserving pseudo-potentials and

[a] *Current Address*: Physics Department, University of Texas at Austin, Austin, Texas 78712, USA.
[b] e-mail: akr@uta.edu

geometry optimizations were performed by Car-Parrinello molecular dynamics techniques. For $C_{40}Si_{20}$, the most stable arrangements correspond to structures in which Si and C atoms form two distinct homogeneous sub-networks and their results, in general, indicate that stable configurations can be achieved provided C and Si atoms do not share the same regions in the cage.

Stabilization of silicon fullerene-like cages with dopant atoms inside has actually been a major field of study in the last few years. The major goal is two-fold: the first is to design silicon based nanostructures with potential applications like carbon fullerenes; and the second is to study *possible* magnetic properties of these structures. The second property might be particularly important in memory devices though it has been noted that silicon cages can almost quench the magnetic moments of transition metal atoms encapsulated in the cage [23]. Recent studies have shown that highly stable small silicon cage clusters are possible if transition metal atoms are encapsulated in the Si cages [13,24]. Bigger clusters like stable Si_{60} fullerene like cages are possible by doping magic clusters such as $Al_{12}X$ (X = Si, Ge, Sn, Pb), Ba@Si_{20} and $Au_{12}W$ inside the Si_{60} cage [25].

The combinations of silicon and carbon atoms in a cluster have generated a significant number of studies on carbon-rich structures in fields ranging from cluster science to astrophysics [26]. Studies have been reported for C_{60} inside a Si_{60} fullerene-like cage which yielded a highly distorted structure [25]. Silicon carbide cluster studies have been mostly focused on carbon rich cage type clusters and, to the best of our knowledge, silicon-rich cage type silicon carbide clusters have *not* been investigated *in detail* so far. We have shown previously using both Hartree-Fock based second order Møller-Plesset perturbation theory and gradient corrected density functional theory (GGA-DFT) that carbon atoms trapped in medium size silicon clusters (Si_n, $n = 8-14$ and 20) produce fullerene- and tube-like nanostructures which are comparable in stability to the transition metal encapsulated silicon cage clusters [27]. We have also reported GGA-DFT results [28] on stabilizing the Si_{60} cage by adding two, four and six carbon atoms inside the cage as well as on the surface of the Si cage by substituting the surface Si atoms. In this paper, we report our results on stabilizing the Si_{60} cage by adding C_{20} and C_{24} clusters inside them ($Si_{60}C_{20}$, $Si_{60}C_{24}$) and also by substitution of silicon atoms by twenty and twenty four carbon atoms on the surface of the cages ($Si_{40}C_{20}$, $Si_{36}C_{24}$) at different possible orientations. As before, the generalized gradient approximation to density functional theory has been used with Perdew-Wang (PW91) exchange-correlation functional [29]. Full geometry optimizations of the cages have been performed without any symmetry constraints with the LANL2DZ basis set [30] and the *Gaussian 03* suite of programs [31]. In this set, for the silicon atom, the Hay-Wadt pseudopotential with the associated basis set are used for the core electrons and the valence electrons, respectively. For the carbon atom, the Dunning/Huzinaga double zeta basis set is employed. All computations have been performed at the supercomputing facilities at the University of Texas at Arlington.

2 Results and discussions

In the first step, silicon atoms on the surface of the cage have been replaced by twenty and twenty four carbon atoms at various symmetry orientations. In the second step, C_{20} and C_{24} clusters were put inside the Si_{60} cage individually. For C_{20} cluster, possible structures reported by theoretical and experimental studies are the bowl, fullerene, ring, bow-tie and planar sheet like structures [19,32]. For C_{24} clusters, theoretical and experimental studies have reported flat graphitic sheet, one pentagon bowl, three pentagon bowl, ring, fullerene and a cage with square, pentagonal and hexagonal faces as possible structures [32]. All these structures, as optimized at GGA-DFT level of theory, have been added inside the Si_{60} cage individually, and then the cage was relaxed altogether.

In the results to follow, we report the electronic states, binding energies per atom (BE), highest occupied — lowest unoccupied molecular orbital (HOMO-LUMO) gaps, vertical ionization potentials (VIPs), vertical electron affinities (VEAs) and total dipole moments of the stable fullerene-like $Si_{40}C_{20}$, $Si_{60}C_{20}$, $Si_{36}C_{24}$ and $Si_{60}C_{24}$ optimized structures with their corresponding average Si–C and C–C bond lengths. Binding energies per atom of the clusters are calculated as the relative energies of these clusters in the separated atom limit, with the atoms in their respective ground states. A positive binding energy thus implies a stable cluster. VIPs and VEAs have been calculated as the difference in the total energies between the neutral clusters and the corresponding positively and negatively charged clusters, respectively, at the neutral optimized geometries. Bonding between the atoms, especially Si–C and C–C for all the stable structures were analyzed using the **N**atural **B**onding **O**rbital (NBO) program and NBO View [33].

We first discuss the C_{20} substitution on the surface of Si_{60} cage. The optimized geometries of all these structures are shown in Figure 1 and their binding energies and other electronic properties are reported in Table 1. The column under the 'structures' in Table 1 refers to the positions of carbon atoms substituting silicon atoms on the surface of Si_{60} cage. The most stable structure Sur1 (Fig. 1a) has twenty carbon atoms in an arrangement of one pentagon surrounded by five hexagons. The structure Sur2 (Fig. 1b) has one hexagon surrounded by three hexagons and three pentagons. The structure Sur3 (Fig. 1c) denotes the other possible way of arranging twenty carbon atoms in the same number of hexagons and pentagons as Sur2. The structures Tb1 (Fig. 1d) and Tb2 (Fig. 1e) have ten carbon atoms along the corners of two hexagons and two pentagons at the two ends of the cage, respectively. For the Dia (Fig. 1f) structure, the twenty carbon atoms are arranged such that the cage is dissected into two sections of Si_{20} (one pentagon surrounded by five hexagons).

As seen from Table 1 for the set of $Si_{40}C_{20}$ clusters, the first three structures are comparable in stability as

Table 1. Binding energy per atom (BE), HOMO-LUMO gap, VEA, VIP (all in eV), dipole moment (Debye), average Si–C bond length (Å) and C–C bond length (Å) for optimized $Si_{40}C_{20}$ fullerene like nanostructures.

Structures	State	BE per atom (eV)	HOMO-LUMO gap (eV)	VEA (eV)	VIP (eV)	Dipole moment (Debye)	Average Si–C bond length (Å)	Average C–C bond length (Å)
Sur1	^{1}A	4.748	0.528	3.722	6.494	1.36	1.91	1.45
Sur2	^{1}A	4.747	0.453	3.747	6.424	2.90	1.85	1.48
Sur3	^{1}A	4.744	0.354	3.779	6.341	2.99	1.88	1.46
Tb1	^{3}A	4.690	0.150	3.936	6.289	1.93	1.91	1.45
Tb2	^{1}A	4.662	0.347	3.675	6.219	0.33	1.85	1.46
Dia	^{1}A	4.639	0.498	3.673	6.533	0.02	1.89	1.44

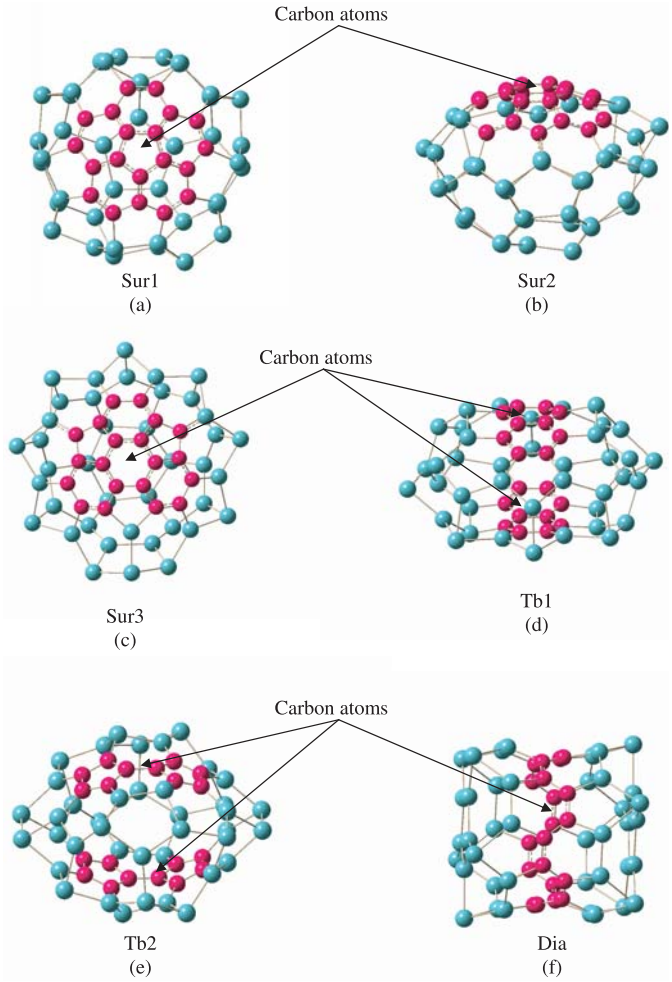

Fig. 1. (Color online) Optimized structures of $Si_{40}C_{20}$ silicon-carbon fullerene like nanostructures (carbon atoms denoted by dark pink color).

their binding energies are within 0.004 eV/atom. The first structure Sur1 has the highest BE per atom in this set, namely 4.748 eV/atom. The dipole moment of this structure has a value of 1.36D, which is the lowest among the top three, indicating less ionic contribution in bonding. The average Si–C and C–C bond lengths for this structure are 1.91 Å and 1.45 Å, respectively. This structure has the highest HOMO-LUMO gap of 0.528 eV and second highest VIP of 6.494 eV in this set. NBO analysis of this structure yields 25 C–C σ bonds, 10 C–C π bonds and 10 Si–C σ bonds. We find strong covalent bonding between the C–C σ bonds and a slight increase in the asymmetric charge distribution among the C–C π bonds in this structure. The binding energy of Sur2 structure is only 0.001 eV per atom lower than the binding energy of the previous structure. NBO analysis yields 24 C–C σ bonds, 8 C–C π bonds, 10 Si–C σ bonds and 3 Si–C π bonds. The number of C–C bonds is lower compared to the previous structure, contributing to the very small difference in binding energy. For Sur3 structure, NBO analysis yields 25 C–C σ bonds, 10 C–C π bonds and 10 Si–C σ bonds. These numbers are similar to the Sur1 structure but the average occupancies of the C–C π bonds and the Si–C σ bonds are slightly lower, indicating weaker C–C and Si–C interactions. These contribute to the lower binding energy. For the other three structures in Table 1, the binding energies are lower mainly due to the lower number of C–C σ- and π-bonds. For the Dia structure though the number of Si–C σ bonds is the highest, smaller number of C–C bonds lowers its stability compared to the other clusters. This structure has the highest VIP and the lowest dipole moment in this set.

The second set of optimized structures, $Si_{60}C_{20}$ with C_{20} clusters inside the Si_{60} cage, is listed in Table 2 and the corresponding geometries are presented in Figure 2. Here also the column below the structures denotes the orientations of carbon atoms inside the Si_{60} cage. The bowl structure (Fig. 2a) has a C_{20} bowl (one pentagon surrounded by five hexagons) inside the Si_{60} cage. The Sheet2 structure (Fig. 2b) has twenty carbon atoms in four hexagons and one heptagon (in a flat sheet like arrangement) inside the Si_{60} cage. For the Sheet1 structure (Fig. 2c), there are twenty carbon atoms in five hexagons (in a flat sheet like arrangement) inside the Si_{60} cage. The Cage (Fig. 2d) has C_{20} cluster in a fullerene like cage arrangement and the Ring (Fig. 2e) has C_{20} cluster in a ring arrangement inside the Si_{60} cage. We also put carbon atoms closer to the surface, with the same surface orientations in Table 1, at an initial optimized SiC dimer bond length of 1.77 Å (at the GGA-DFT level of theory) but the optimized structures were energetically unfavorable.

The bowl structure has the highest BE per atom of 4.482 eV and also the highest VIP in this set. The dipole moment value of 2.73D indicates a mixed

Table 2. Binding energy per atom (BE), HOMO-LUMO gap, VEA, VIP (all in eV), dipole moment (Debye), average Si–C bond length (Å) and C–C bond length (Å) for optimized $Si_{60}C_{20}$ fullerene like nanostructures.

Structures	State	BE per atom (eV)	HOMO-LUMO gap (eV)	VEA (eV)	VIP (eV)	Dipole moment (Debye)	Average Si–C bond length (Å)	Average C–C bond length (Å)
Bowl	^{5}A	4.482	0.163	4.105	6.282	2.73	1.94	1.46
Sheet2	^{1}A	4.454	0.159	3.995	6.162	3.86	1.93	1.43
Sheet1	^{1}A	4.434	0.153	4.044	6.233	4.42	1.93	1.43
Cage	^{1}A	4.349	0.109	4.153	6.281	0.02	2.06	1.50
Ring	^{1}A	4.306	0.321	3.832	6.174	2.67	1.99	1.40

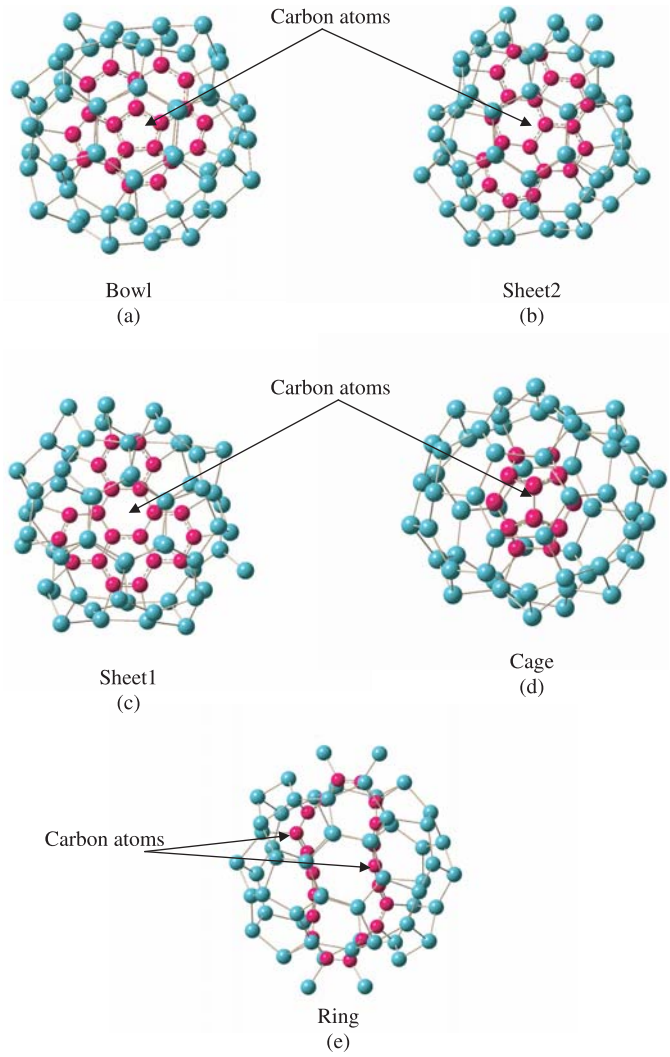

Fig. 2. (Color online) Optimized structures of $Si_{60}C_{20}$ silicon-carbon fullerene like nanostructures (carbon atoms denoted by dark pink color).

ionic-covalent bonding contributing to its increased stability. NBO analysis of this structure yields 25 C–C σ bonds, 11 C–C π bonds and 10 Si–C σ bonds. This structure has the maximum number of C–C bonds, which might be the reason for its increased stability. For the right orientation, the C_{20} bowl was rotated inside the Si_{60} cage at different angles and the variations in the binding energies of the optimized structures were very low, ranging from −0.2% to +0.06%. This indicates a flat potential energy surface with respect to the angle of rotation. The NBO analysis of Sheet2 structure yields 24 C–C σ bonds, 10 C–C π bonds and 12 Si–C σ bonds clearly indicating that a decrease in the number of C–C bonds contributes to a lower binding energy. NBO analysis of Sheet1 structure yields the same number of C–C and Si–C bonds as Sheet2 structure but the average occupancies of the bonds were lower contributing to the lower binding energy. The Cage structure has the lowest dipole moment of 0.02D indicating higher covalent bonding. However, the NBO analysis of the Cage structure yields the maximum number of 30 C–C σ bonds and 6 C–C π bonds but the number of Si–C σ bonds were four and also weaker. The average Si–C bond length, which is the highest from Table 2, clearly indicates that the lower number and the weaker Si–C interaction contribute to its lower stability. The Cage structure has the highest VEA in Table 2. There is a sudden increase in the HOMO-LUMO gap in Table 2 for the Ring structure. This gap is comparable to the gaps of Table 1. This may be due to the fact that some of the carbon atoms reach to the surface of Si cage, thereby nearly displacing those surface Si atoms, as seen from Figure 2e. For the Ring structure though the number of Si–C σ bonds is maximum (a total of 18), the average occupancies of Si–C bonds were lower compared to all the previous structures.

The third set of optimized structures is $Si_{36}C_{24}$ fullerene like nanostructures, which have twenty four carbon atoms substituting the silicon atoms on the surface of the Si_{60} cage. These are reported in Table 3 and their corresponding relaxed geometries are presented in Figure 3. The structure Sur4 (Fig. 3a) has twenty four carbon atoms arranged along the corners in four pentagons and four hexagons. The structures Sur1 (Fig. 3b), Sur2 (Fig. 3d) and Sur3 (Fig. 3e) have the basic prototype of one pentagon surrounded by five hexagons for twenty carbon atoms, differing in the arrangement of other four carbon atoms. For the structure Sur5 (Fig. 3c), there are twenty four carbon atoms along the corners of three pentagons and five hexagons. The rest of the structures Tb4 (Fig. 3f), Tb2 (Fig. 3g), Tb3 (Fig. 3h), Tb1 (Fig. 3i) and Tb5 (Fig. 3j) have twelve carbon atoms in different arrangements along the two ends of the cage.

For the first five structures in Table 3, the binding energies per atom are within 10 meV. So these five structures are comparable in stability. The Sur4 structure has

Table 3. Binding energy per atom (BE), HOMO-LUMO gap, VEA, VIP (all in eV), dipole moment (Debye), average Si–C bond length (Å) and C–C bond length (Å) for optimized $Si_{36}C_{24}$ fullerene like nanostructures.

Structures	State	BE per atom (eV)	HOMO-LUMO gap (eV)	VEA (eV)	VIP (eV)	Dipole moment (Debye)	Average Si–C bond length (Å)	Average C–C bond length (Å)
Sur4	^{1}A	4.977	0.557	3.621	6.450	1.41	1.84	1.46
Sur1	^{1}A	4.975	0.531	3.617	6.456	0.72	1.84	1.47
Sur5	^{1}A	4.975	0.486	3.733	6.661	1.66	1.87	1.46
Sur2	^{1}A	4.971	0.332	3.662	6.282	1.16	1.90	1.45
Sur3	^{1}A	4.967	0.406	3.635	6.339	1.09	1.85	1.47
Tb4	^{1}A	4.960	0.277	3.479	6.154	0.01	1.89	1.45
Tb2	^{1}A	4.932	0.371	3.647	6.262	0.72	1.85	1.46
Tb3	^{1}A	4.920	0.574	3.565	6.401	0.01	1.89	1.45
Tb1	^{1}A	4.867	0.430	3.534	6.201	0.01	1.85	1.47
Tb5	^{1}A	4.851	0.525	3.526	6.242	0.00	1.87	1.47

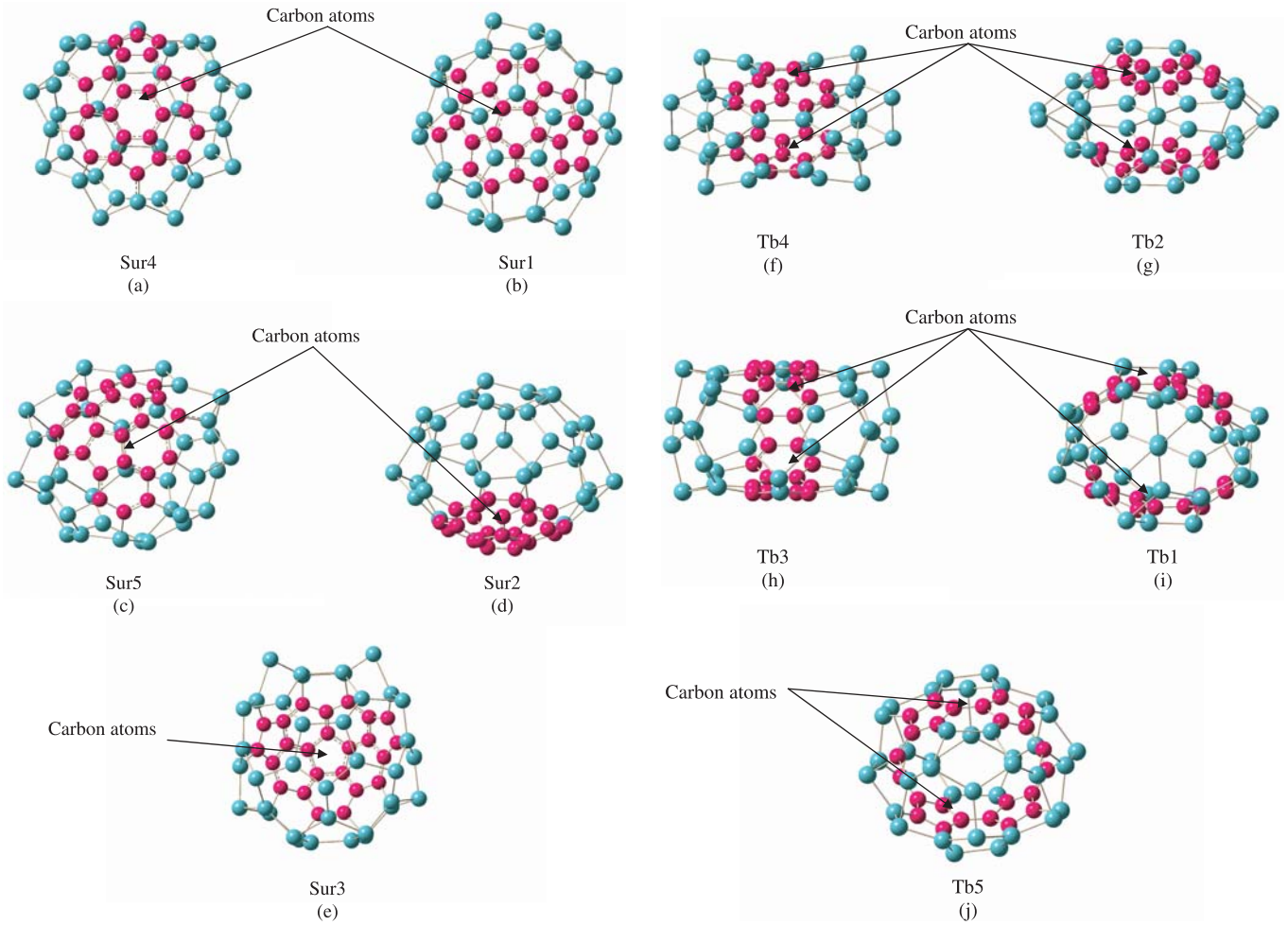

Fig. 3. (Color online) Optimized structures of $Si_{36}C_{24}$ silicon-carbon fullerene like nanostructures (carbon atoms denoted by dark pink color).

the highest BE per atom of 4.977 eV and has the highest HOMO-LUMO gap of 0.557 eV in this set. The dipole moment value of 1.41D indicates a mixed ionic-covalent bonding nature contributing to its stability. NBO analysis of this structure yields 31 C–C σ bonds, 10 C–C π bonds, 10 Si–C σ bonds and 4 Si–C π bonds. Both the next two structures Sur1 and Sur5 differ in BE per atom by 0.002 eV compared to Sur4 structure. NBO analysis for Sur1 structure yields 30 C–C σ bonds, 11 C–C π bonds, 12 Si–C σ bonds and 2 Si–C π bonds. One of the reasons for its lower binding energy might be the substitution of a C–C σ bond by a C–C π bond having lower occupancy. NBO analysis of Sur5 structure yields 31 C–C σ bonds, 11 C–C π bonds, 10 Si–C σ bonds and 2 Si–C π bonds.

Table 4. Binding energy per atom (BE), HOMO-LUMO gap, VEA, VIP (all in eV), dipole moment (Debye), average Si–C bond length (Å) and C–C bond length (Å) for optimized $Si_{60}C_{24}$ fullerene like nanostructures.

Structures	State	BE per atom (eV)	HOMO-LUMO gap (eV)	VEA (eV)	VIP (eV)	Dipole moment (Debye)	Average Si–C bond length (Å)	Average C–C bond length (Å)
Sheet	^{3}A	4.599	0.100	4.142	6.222	2.15	1.91	1.42
3bowl	^{1}A	4.579	0.209	4.130	6.292	2.21	1.95	1.44
1bowl	^{1}A	4.566	0.252	4.013	6.287	3.11	1.93	1.43
Cage	^{3}A	4.529	0.202	4.132	6.272	0.75	2.02	1.53
Rcage	^{5}A	4.487	0.016	4.094	6.179	0.07	2.06	1.53
Ring	^{3}A	4.358	0.112	4.106	6.143	0.59	1.91	1.44

The number of C–C bonds is one more than the Sur4 structure but the Si–C interactions were lower, contributing to its lower stability. This might indicate that Si–C interactions are also important for the stability of these nanostructures. This structure has the highest VIP and VEA in this set. For Sur2 structure, NBO analysis yields 30 C–C σ bonds, 12 C–C π bonds and 12 Si–C σ bonds but the Si–C interactions were weaker (average Si–C bond length of 1.90 Å) contributing to its lower stability. The set of structures Tb4, Tb2, Tb3, Tb1 and Tb5 have twelve carbon atoms along the two ends of the cage, indicating that the number of Si–C interactions is higher and the number of C–C interactions is lower compared to the previous structures. Less C–C interactions contribute to their low binding energies. Except for the Tb2 structure, the dipole moment values for the rest of the structures indicate very negligible ionic contribution and strong covalent bonding. Important thing to be noted in the Tb4 structure is that the optimized structure shows significant reconstructions from its original fullerene like geometry to a flat tube like geometry.

The last set of optimized structures is $Si_{60}C_{24}$ fullerene like nanostructures, which has C_{24} clusters inside the Si_{60} cage. These are reported in Table 4 and the corresponding geometries are shown in Figure 4. The Sheet structure (Fig. 4a) has twenty four carbon atoms placed on the corners of seven hexagons (in a flat sheet like arrangement) inside the Si_{60} cage. In 3bowl structure (Fig. 4b) carbon atoms are arranged among three pentagons and five hexagons inside the Si_{60} cage. For 1bowl structure (Fig. 4c), twenty four carbon atoms are arranged among one pentagon and six hexagons inside the Si_{60} cage. The Cage (Fig. 4d), Rcage (Fig. 4e) and Ring (Fig. 4f) structures have C_{24} clusters inside the Si_{60} cage in fullerene like cage, square cage (having pentagonal, hexagonal and square faces) and ring like arrangements, respectively. As in $Si_{40}C_{20}$, here also we put the carbon atoms closer to the surface from inside the cage at an initial optimized SiC dimer bond length, but the optimized structures were found to be energetically unfavorable.

The Sheet structure has the highest BE per atom of 4.599 eV and also highest VEA of 4.142 eV in this set. The dipole moment value of 2.15D indicates a mixed ionic-covalent bonding nature contributing to its stability. NBO analysis of this structure yields 30 C–C σ bonds, 13 C–C π bonds and 12 Si–C σ bonds. NBO analysis

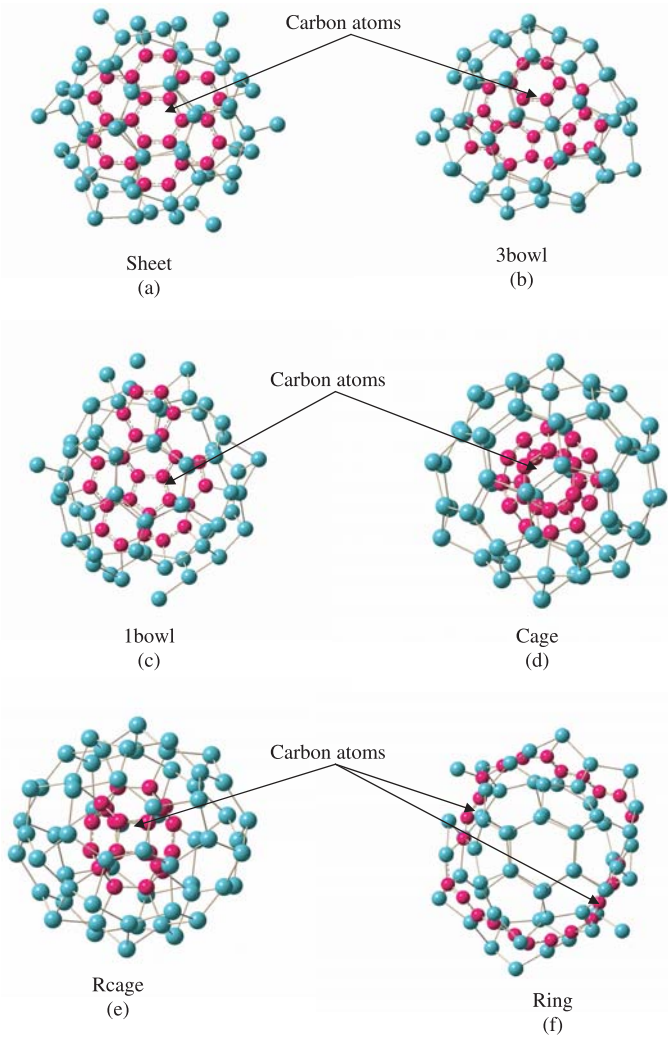

Fig. 4. (Color online) Optimized structures of $Si_{60}C_{24}$ silicon-carbon fullerene like nanostructures (carbon atoms denoted by dark pink color).

of the 3bowl structure yields 31 C–C σ bonds, 11 C–C π bonds and 12 Si–C σ bonds. The total number of C–C bonds in this structure is lower compared to previous structure. The average occupancies of C–C π bonds and Si–C σ bonds are also lower compared to the previous structure. These might be the reasons for 3bowl structure to have lower binding energy compared to Sheet

structure. NBO analysis of the 1bowl structure yields 30 C–C σ bonds, 12 C–C π bonds and 12 Si–C σ bonds. One of the C–C σ bonds in the 3bowl structure is replaced by a C–C π bond in the 1bowl structure with occupancy lower compared to σ bond and resulting lower stability for the 1bowl structure compared to the 3bowl structure. For the Cage structure, NBO analysis yields maximum number of C–C bonds in this set (36 σ bonds and 8 π bonds) but the number of Si–C bonds (11 σ bonds) were lower and also weaker. The C–C interactions are also weaker for this structure (average C–C bond length of 1.53 Å). This clearly indicates that both Si–C and C–C bonding are important for stability. The Rcage structure also has weaker Si–C interactions, as evident from the average Si–C bond length similar to the Cage structure. The number of C–C bonds is also lower in this structure (36 σ bonds and 6 π bonds) compared to Cage structure. It is to be noted that the HOMO-LUMO gap for the Rcage structure is 0.016 eV, indicating almost a metallic behavior. NBO analysis of the Ring structure yields the maximum number of Si–C bonds (28 σ bonds) and minimum number of C–C bonds (22 σ bonds and 12 π bonds) in this set. In this structure, all carbon atoms came to the surface of the cage by displacing surface silicon atoms, thereby creating a highly distorted cage with broken carbon chain. This results in lower number of C–C bonds and a lower binding energy for the cage.

A common feature of the above $Si_{60}C_{24}$ structures is that the carbon atoms put inside the Si_{60} cage interact with the silicon atoms on the surface and push a few silicon atoms outside the surface of the cage, and as a result those silicon atoms become loosely bound to the cage. This might be one of the reasons for the lower binding energy of these set compared to $Si_{36}C_{24}$ nanostructures. For example, let us compare the 1bowl structure with the Sur2 structure (Fig. 3d), where the arrangements of carbon atoms in both the structures are the same and are inside and at surface of the cage, respectively. NBO analysis of this Sur2 structure yields 30 C–C σ bonds, 12 C–C π bonds and 12 Si–C σ bonds similar to the 1bowl ($Si_{60}C_{24}$) structure. The average occupancies of the C–C π bonds and the Si–C σ bonds were higher for Sur2 cage, contributing to its increased binding energy. This might again indicate that both Si–C and C–C interactions are important for stability and their interactions are stronger at the surface than inside the cage. In fact, the increase in Si–C bonding at the expense of C–C bonding contributes to lower stability. For example, in the Ring structure, with the maximum number of Si–C bonds (28 σ bonds), the number of and C–C bonds are lower (22 σ bonds and 12 π bonds) leading to lower stability.

Similar conclusions can be reached for the set of $Si_{60}C_{20}$ and $Si_{40}C_{20}$ nanostructures. From Table 2, the structure Sheet1 (Fig. 2c) BE per atom differs from the most stable structure by 0.048 eV. NBO analysis of this structure yields 24 C–C σ bonds, 10 C–C π bonds and 12 Si–C σ bonds. NBO analysis for the most stable Bowl structure in this set yields 25 C–C σ bonds, 11 C–C π bonds and 11 Si–C σ bonds, clearly indicating that increased Si–C and C–C interactions contributed to its higher binding energy. The arrangements of twenty carbon atoms are the same for the Bowl structure and the most stable Sur1 structure ($Si_{40}C_{20}$) from Table 1. As mentioned before, NBO analysis of this Sur1 structure yields 25 C–C σ bonds, 10 C–C π bonds and 10 Si–C σ bonds. This structure has one less C–C π bond and one less Si–C σ bond compared to those of the Bowl structure ($Si_{60}C_{20}$). The average occupancies of C–C π bond (1.70) and Si–C σ bond (1.94) in this Sur1 structure are greater than the most stable Bowl Structure (1.67 and 1.89 respectively), clearly indicating stronger Si–C interactions and C–C interactions at the surface contributing to its higher binding energy.

In general, all the optimized structures considered here are stable nanostructures with higher binding energies per atom compared to the bare Si_{60} cage which has a binding energy per atom of 3.61eV at GGA-DFT level of theory. In addition, all harmonic frequencies of the most stable structures are found to be positive. In our previous work [28], we have seen that binding energies per atom for the $Si_{60-2n}C_{2n}$ and $Si_{60}C_{2n}$ ($n = 1$ to 3) fullerene like nanostructures were higher compared to the bare Si_{60} cage and they increase with the number of carbon atoms from two to six. Also, the structures with carbon atoms substituting silicon atoms on the surface of the Si_{60} fullerene cage give higher binding energies compared to the structures with carbon atoms inside the Si_{60} cage. Here also we note from Tables 1 to 4 that the binding energies of $Si_{40}C_{20}$, $Si_{60}C_{20}$, $Si_{36}C_{24}$ and $Si_{60}C_{24}$ nanostructures are higher compared to our previous results for two, four and six carbon atoms and agree with the trend of increasing binding energies with the increase in the number of carbon atoms. The stabilities of the nanostructures here are found to be dependent on the orientations of the carbon atoms inside or on the surface of fullerene like cage. All the optimized nanostructures tend to be distorted and do not show a trend of smoother fullerene like silicon nanostructures.

As mentioned before that for the most part carbon-carbon interactions and the Si–C interactions contribute to fullerene cage stability. The inclusion of twenty carbon atoms on the surface of the Si_{60} cage increased the BE per atom by 31.5% and the inclusion of twenty carbon atoms inside the Si_{60} cage increased BE per atom by 24% compared to the BE of the bare Si_{60} cage. For twenty four carbon atoms on the surface of the cage and inside the cage, the BE per atom increased by 38% and 27% compared to the BE of the bare Si_{60} cage. This indicates that Si–C bonding is stronger at the surface than inside the cage. This could be evident from the fact that inclusion of carbon atoms inside the Si_{60} cage pushes silicon atoms outside the surface, which are then loosely bonded to the cage. These results are, in general, consistent with the results of Matsubara and Massobrio who observed that for carbon-rich carbon-silicon fullerenes stable configurations can be achieved provided C and Si atoms do not share the same regions in the cage [22].

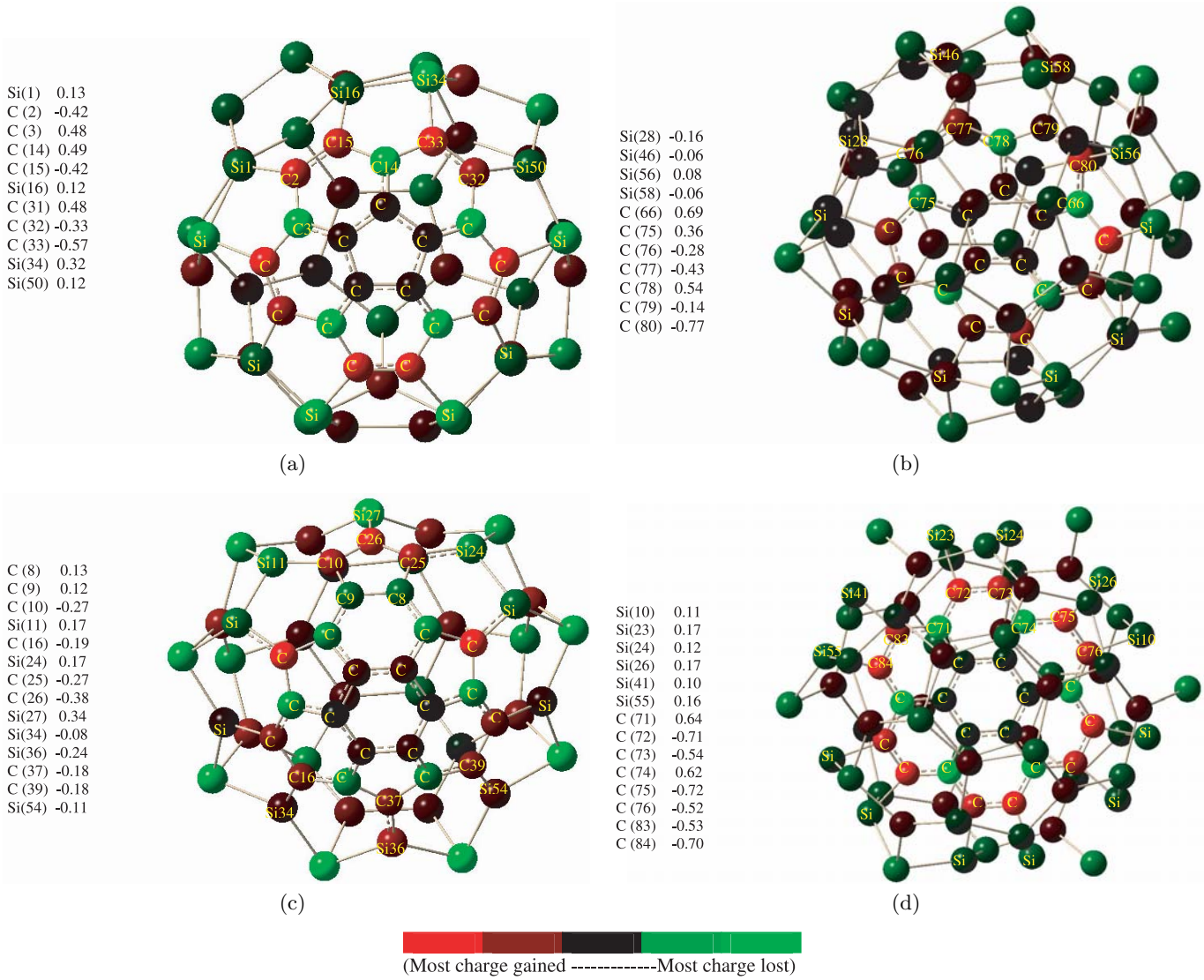

Fig. 5. (Color online) Mulliken charge distribution for: the most stable Sur1 ($Si_{40}C_{20}$) structure (a); the most stable Bowl ($Si_{60}C_{20}$) structure (b); the most stable Bowl ($Si_{36}C_{24}$) structure (c); the most stable Sheet ($Si_{60}C_{24}$) structure (d). Selected atom labels with their respective electronic charge shown in the figure.

We also performed detailed Mulliken population analysis for the clusters reported here. In general, Mulliken charge analysis for all the structures indicates that carbon atoms gain charge and the silicon atoms lose charge, as expected from their electro-negativities. Some exceptions are noted in which carbon atoms lose charge and silicon atoms gain charge indicating an asymmetric charge distribution and a total dipole moment for these structures. Mulliken charge distribution diagrams for the four most stable structures in each set along with the electronic charges for selective group of atoms are shown in Figures 5a–5d. All the charges are noted in electronic charge unit. In general, these most stable structures have mostly covalent and partly ionic bonding. Increase in the exceptions of silicon atoms gaining charge translates to increased repulsive interaction between them and carbon atoms, resulting in a decrease of stability. For example, in the $Si_{40}C_{20}$ Sur1 structure (Fig. 5a) we notice that the five inner-most carbon atoms and few outer carbon atoms have positive electronic charges and this induces the ionic contribution over the covalent bonding between the carbon atoms. Electronic charges for selective atom labels for this structure are given in Figure 5a. All the silicon atoms bonded with carbon atoms have positive electronic charges and the asymmetric charge distribution between the silicon and carbon atoms increases the asymmetric contribution between the C–C bonding. For the most stable $Si_{60}C_{20}$ Bowl structure (Fig. 5b), we notice several exceptions where silicon atoms gain charges, while five carbon atoms lose charges. Some silicon atoms bonded with carbon atoms gain charge similar to carbon atoms, increasing the repulsive Coulombic interaction between the silicon and carbon atoms. Electronic charges for selective atom labels for this structure are given in Figure 5b. For

example the silicon atoms (labels 28, 46, 58) having electronic charges of −0.16, −0.06 and −0.06 respectively are bonded with carbon atoms (labels 76, 77 and 79) having electronic charges of −0.28, −0.43 and −0.14, which indicates the repulsive interaction between the silicon and carbon atoms offsetting the increased C–C interaction, lowering the stability for this structure. NBO analysis confirms the ionic contribution to the C–C interaction among the C–C π bonds with C–C σ bonds being strongly covalent in nature. Similar discussions can be made for the most stable $Si_{36}C_{24}$ and $Si_{60}C_{24}$ fullerene like nanostructures. The VIPs and the VEAs for all the optimized nanostructures reported in this work are considerably high indicating stability and do not follow any specific pattern with increase in carbon atoms. In general, Mulliken charge analysis for the novel silicon-carbon fullerene like nanostructures ($Si_{40}C_{20}$, $Si_{60}C_{20}$, $Si_{36}C_{24}$ and $Si_{60}C_{24}$) indicates a mixed ionic-covalent bonding contributing to the stability.

3 Conclusions

In conclusion, we have studied a class of stable $Si_{40}C_{20}$, $Si_{60}C_{20}$, $Si_{36}C_{24}$ and $Si_{60}C_{24}$ fullerene-like nanostructures. These structures have increased stability compared to the bare Si_{60} cage and their stability depends on the orientation of carbon atoms inside or on the surface of the cage. The ground state structures for twenty and twenty four carbon atoms on the surface of the cage are in singlet state, i.e., no magnetic structures have been found. For C_{20} and C_{24} clusters inside the Si_{60} cage, the ground state structures have multiplicities of 5 and 3 indicating the possibility of magnetic nanostructures. Further studies are needed to ascertain probable magnetism associated with these structures. For twenty and twenty four carbon atoms on the surface and inside the Si_{60} cage, a mixed ionic-covalent bonding contributed to the stability. The C–C interactions and Si–C interactions together contribute to the stability of $Si_{40}C_{20}$, $Si_{60}C_{20}$, $Si_{36}C_{24}$ and $Si_{60}C_{24}$ fullerene like nanostructures. Both C–C interactions and Si–C interactions were stronger on the surface than inside the cage which is evident from the fact that $Si_{40}C_{20}$ and $Si_{36}C_{24}$ nanostructures have higher binding energies compared to $Si_{60}C_{20}$ and $Si_{60}C_{24}$ nanostructures. This conclusion can also be supported by the fact that increase in binding energies for most stable structures in $Si_{40}C_{20}$ and $Si_{36}C_{24}$ (compared to bare Si_{60} cage) were 31.5% and 38% compared to 24% and 27% for $Si_{60}C_{20}$ and $Si_{60}C_{24}$ nanostructures, respectively. Thus the orientations of twenty and twenty four carbon atoms on the surface are found to have larger impact on the stability of the Si_{60} cage. All these along with the fact that closed cage carbon clusters put at the center of the cage (having weaker Si–C interactions) do not contribute to higher stability, suggest that as carbon atoms are increased in the cage, the local Si–C interactions and C–C interactions are the dominant factors in deciding the stability of the clusters. Hence we may suggest that proper arrangements with more carbon atoms might be needed to have a more stabilized and smoother fullerene-like silicon nanostructure. Significant reconstructions shown by some $Si_{36}C_{24}$ nanostructures with optimized geometries looking like a flat tube structure indicates the possibility of Si–C nanotubes. Further theoretical and experimental studies are needed to explore this possibility. We have stated before that, to the best of our knowledge, *no* experimental results are available for the SiC fullerene structures reported here. Further theoretical and *new* experimental studies are clearly necessary to understand the hybrid nature of bonding and the stability of the nanostructure fullerene cages reported in this study.

The authors gratefully acknowledge partial support from the Welch Foundation, Houston, Texas (Grant Nos. Y-1525 and F-0934). We also appreciate very useful comments from the referees.

References

1. *Atomic and Molecular Clusters*, edited by E.R. Bernstein (Elsevier, New York, 1990)
2. *Physics and Chemistry of Finite Systems – From Clusters to Crystals, Proceedings of the NATO Advanced Research Workshop*, edited by P. Jena, S.N. Khanna, B.K. Rao (Kluwer Academic Publishing, 1991); *Theory of Atomic and Molecular Clusters* (Springer-Verlag, Berlin, 1999)
3. *Clusters of Atoms and Molecules*, edited by H. Haberland (Springer-Verlag, Berlin, 1994)
4. U. Naher, S. Bjornholm, S. Frauendorf, F. Garcias, C. Guet, Phys. Rep. **285**, 245 (1997)
5. S. Sugano, H. Koizumi, *Microcluster Physics* (Springer-Verlag, New York, 1998)
6. *Theory of Atomic and Molecular Clusters: With a Glimpse at Experiments,* edited by J. Jellinek, R.S. Berry, J. Jortner (Springer-Verlag, New York, 1999)
7. S. Bjornholm, J. Borggreen, Philos. Mag. B **79**, 1321 (1999)
8. Roy L. Johnston, R.L. Johnston, *Atomic and Molecular Clusters* (Routledge Publishing, New York, 2002)
9. *Encyclopedia of Nanoscience and Nanotechnology*, edited by H.S. Nalwa (American Scientific Publishers, California, 2004)
10. F. Baletto, R. Ferrando, Rev. Mod. Phys. **77**, 371 (2005)
11. N.E. Frick, *An Ab Initio Study of Alkali – C_{60} Complexes*, M.S. thesis, The University of Texas at Arlington, May 2002 and references therein; N.E. Frick, A.S. Hira, A.K. Ray, in preparation
12. R.-H. Xie, G.W. Bryant, J. Zhao, V.H. Smith Jr, A.D. Carlo, A. Pecchia, Phys. Rev. Lett. **90**, 206602 (2003); R.–H. Xie, G.W. Bryant, G. Sun, T. Kar, Z. Chen, V.H. Smith Jr, Y. Araki, N. Tagmatarchis, H. Shinohara, O. Ito, Phys. Rev. B **69**, 201403 (2004)
13. H. Hiura, T. Miyazaki, T. Kanayama, Phys. Rev. Lett. **86**, 1733 (2001); T. Miyazaki, H. Hiura, T. Kanayama, Phys. Rev. B **66**, 121403 (R) (2002)
14. A. Szabo, N.S. Ostlund, *Modern Quantum Chemistry* (Macmillan, New York, 1982)
15. W.J. Hehre, P.v.R. Schleyer, J.A. Pople, *Ab Initio Molecular Orbital Theory* (Wiley, New York, 1982)

16. R.G. Parr, W. Yang, *Density Functional Theory of Atoms and Molecules* (Oxford University Press, New York, 1989)
17. K.-M. Ho, A.A. Shvartsburg, B. Pan, Z.-Y. Lu, C.-Z. Wang, J. G. Wacker, J.L. Fye, M.F. Jarrold, Nature **392**, 582 (1998)
18. G.V. Helden, M.T. Hsu, N. Gotts, M.T. Bowers, J. Phys. Chem. **97**, 8182 (1993)
19. M.F. Jarrold, Nature **407**, 26 (2000); J. C. Grossman, L. Mitas, K. Raghavachari, Phys. Rev. Lett. **75**, 3870 (1995)
20. B.-X. Li, P.-L. Cao, D.-L. Que, Phys. Rev. B **61**, 1685 (2000); B.-X. Li, P.-L. Cao, B. Song, Z.-Z. Ye, J. Mol. Struct. (Theochem) **620**, 189 (2003); M.C. Piqueras, R. Crespo, E. Orti, F. Tomas, Chem. Phys. Lett. **213**, 509 (1993); R. Crespo, M.C. Piqueras, F. Tomas, Synth. Met. **77**, 13 (1996); K. Jug, M. Krack, Chem. Phys. **173**, 439 (1993); F.S. Khan, J.Q. Broughton, Phys. Rev. B **43**, 11754 (1991); Z. Chen, H. Jiao, G. Seifert, A.H.C. Horn, D. Yu, T. Clark, W. Thiel, P.V.R. Schleyer, J. Comp. Chem. **24**, 948 (2003); M. Menon, K.R. Subbaswamy, Chem. Phys. Lett. **219**, 219 (1994)
21. M. Menon, J. Chem. Phys. **114**, 7731 (2001)
22. M. Matsubara, C. Massobrio, J. Phys. Chem. A **109**, 4415 (2005)
23. S. N. Khanna, B.K. Rao, P. Jena, Phys. Rev. Lett. **89**, 016803 (2002); W. Zheng, J.M. Nilles, D. Radisic, K.H. Bowen, J. Chem. Phys. **122**, 071101 (2005)
24. K. Jackson, B. Nellermoe, Chem. Phys. Lett. **254**, 249 (1996); V. Kumar, Y.Kawazoe, Phys. Rev. Lett. **87**, 045503 (2001); Phys. Rev. B **65**, 073404 (2002); H. Kawamura, V. Kumar, Y. Kawazoe, Phys. Rev. B **70**, 245433 (2004); C. Xiao, F. Hagelberg, W.A. Lester, Phys. Rev. B **66**, 075425 (2002); A.K. Singh, V. Kumar, Y. Kawazoe, Phys. Rev. B **71**, 115429 (2005)
25. Q. Sun, Q. Wang, P. Jena, B.K. Rao, Y. Kawazoe, Phys. Rev. Lett. **90**, 135503 (2003); Q. Sun, Q. Wang, P. Jena, J.Z. Yu, Y. Kawazoe, Sci. Tech. Adv. Mats **4**, 361 (2003); Q. Sun, Q. Wang, Y. Kawazoe, P. Jena, Eur. Phys. J. D **29**, 231 (2004)
26. V.D. Gordon, E.S. Nathan, A.J. Apponi, M.C. McCarthy, P. Thaddeus, P. Botschwina, J. Chem. Phys. **113**, 5311 (2000); J. Cernicharo, C.A. Gottlieb, M. Guelin, P. Thaddeus, J.M. Vrtilek, Astrophys. J. **341**, L25 (1989); M. Oshishi, N. Kaifu, K. Kawaguchi, A. Murakami, S. Saito, S. Yamamoto, S.-I. Ishikawa, Y. Fujita, Y. Shiratori, W.M. Irvine, Astrophys. J. **34**, L83 (1989); S. Hunsicker, R.O. Jones, J. Chem. Phys. **105**, 5048 (1996); S. Osawa, M. Harada, E. Osawa, Fullerene Sci. Tech. **3**, 225 (1995); M. Pellarin, C. Ray, J. Lerme, J.L. Vialle, M. Broyer, X. Blase, P. Keghelian, P. Melinon, A. Perez, J. Chem. Phys. **110**, 6927 (1999); C. Ray, M. Pellarin, J.L. Lerme, J.L. Vialle, M. Broyer, X. Blase, P. Keghelian, P. Melinon, A. Perez, Phys. Rev. Lett. **80**, 5365 (1998); W. Branz, I.M.L. Billas, N. Malinowski, F. Tast, M. Heinebrodt, T.P. Martin, J. Chem. Phys. **109**, 3425 (1998); P. Pradhan, A.K. Ray, J. Mol. Struc. (Theochem) **716**, 109 (2004); P. Pradhan, A.K. Ray, Eur. Phys. J. D **37**, 393 (2006)
27. M.N. Huda, A.K. Ray, Phys. Rev. A **69**, 011201 (R) (2004); M.N. Huda, A.K. Ray, Eur. Phys. J. D **31**, 63 (2004)
28. A. Srinivasan, *On the Existence and Stability of Carbon-Based Silicon Fullerenes – A Density Functional Theoretic Study*, M.S. thesis, The University of Texas at Arlington, December 2005; A. Srinivasan, M.N. Huda, A.K. Ray, Phys. Rev. A. **72**, 063201 (2005); A. Srinivasan, A.K. Ray, J. Nanosci. Nanotech. **6**, 43 (2006)
29. J.P. Perdew, K. Burke, Y. Wang, Phys. Rev. B **54**, 16533 (1996); J.P. Perdew, K. Burke, M. Ernzerhof, Phys. Rev. Lett. **77**, 3865 (1996); J.P. Perdew, J.A. Chevary, S.H. Vosko, K.A. Jackson, M.R. Pederson, D.J. Singh, C. Fiolhais, Phys. Rev. B **46**, 6671 (1992); J.P. Perdew, J.A. Chevary, S.H. Vosko, K.A. Jackson, M.R. Pederson, D.J. Singh, C. Fiolhais, Phys. Rev. B **48**, 4978 (1993)
30. P.J. Hay, W.R. Wadt, J. Chem. Phys. **82**, 284 (1985)
31. M.J. Frisch et al., *Gaussian 03* (Revision C.02), Gaussian Inc., Pittsburgh, PA, 2003.
32. R.O. Jones, J. Chem. Phys. **110**, 5189 (1999); L. Turker, J. Mol. Struct. (Theochem) **625**, 169 (2003); P.R.C. Kent, M.D. Towler, R.J. Needs, G. Rajagopal, Phys. Rev. B **62**, 15394 (2000); J.M.L. Martin, J. El-Yazal, J.-P. Francois, Chem. Phys. Lett **255**, 7 (1996); R.O. Jones, G. Seifert, Phys. Rev. Lett. **79**, 443 (1997); J.I. Chavez, M.M. Carrillo, K.A. Beran, J. Comput. Chem. **25**, 322 (2004); A.V. Orden, R.J. Saykally, Chem. Rev. **98**, 2313 (1998); C. Zhang, X. Xu, H. Wu, Q. Zhang, Chem. Phys. Lett. **364**, 213 (2002); W. Cai, N. Shao, X. Shao, Z. Pan, J. Mol. Struct. (Theochem) **678**, 113 (2004); B.R. Eggen, R.L. Johnston, J.N. Murell, J. Chem. Soc. Faraday Trans. **90**, 3029 (1994)
33. E.D. Glendening, J.K. Badenhoop, A.E. Reed, J.E. Carpenter, J.A. Bohmann, C.M. Morales, F. Weinhold, *NBO 5.0*, Theoretical Chemistry Institute, University of Wisconsin, Madison (2001)